

# A systematic computational study to observe the effect on Sb doping on electronic band structure, and optical properties of SnO<sub>2</sub>

Awais Tabassum<sup>1</sup>, Muhammad Khizar Iqbal<sup>\*2</sup>

<sup>1</sup>Joint Laboratory for Extreme Conditions Matter Properties, School of Mathematics and Physics, Southwest University of Science and Technology, Mianyang 621010, P.R. China.

<sup>2</sup>School of Material Science and Engineering, Southwest University of Science and Technology, Mianyang 621010, P.R. China

Email: awaistabassum000@gmail.com (A.T) 1st Author

Email: khizariqbal2525@gmail.com (M.K.I) Corresponding Author

**Abstract-** Among the transparent conducting oxides (TCOs), SnO<sub>2</sub> has been extensively explored due to the following applications: optoelectronic devices, solar cells, light-emitting devices, plasma-screen indicators, and other electronics devices. Hence, in the present investigation, the values of the electronic and optical gaps of the parental and Sb doped SnO<sub>2</sub> (12.5%, 25%, and 37.5%) compound have been computed using the DFT calculations. The parental compounds indicate the semiconducting character, and after doping with Sb, the character of the materials changes to metallic. The band structure of 12.5%, and 25% indicates that two bands cross the Fermi level, whereas the band structure of 37.5% indicates that three bands cross the Fermi level, respectively. It has been noticed that the character of the Oxygen atom is dominant in the Fermi level. The total density of states (DOS) at Fermi level  $E_F$  is 10.3, 15.0, and 14.8 states/eV for 12.5%, 25%, and 37.5%, respectively. From the above calculations, it can also be concluded that the metallic character of the materials can also be observed from the finite DOS at Fermi level. The anisotropic features of the imaginary, and real parts of complex dielectric functions, reflectivity, refractive index, extension coefficient, and energy loss function have been computed along with the component of electric field polarization. From the calculations, it can be stated that the variation in the optical spectra of the three compounds has been observed due to the Sb percentage doping. It has also been observed that the variation in the peaks' height due to the increment of Sb atom percentage, indicating that the 37.5% doped compound has more metallic character than the 12.5%, and 25% doped compounds.

**Keywords:** TCOs, Density functional theory (DFT), Local density approximation, Wien2k code.

## I. INTRODUCTION

The use of Transparent Conducting Oxides (TCOs), which have been widely used and frequently investigated, has a wide scope in the field of optoelectronic devices, including but are restricted to: solar cells, light-emitting diodes, flat panel television, thin-film transistors [1, 2]. The presumably ideal material to use as a TCO is (SnO<sub>2</sub>). In fact, SnO<sub>2</sub> is an intrinsic semiconductor material possessing a wide band gap, appearing to have n-type conductivity. The resistivity could be lowered to  $2.3 \times 10^{-4} \Omega/\text{cm}$  by introducing extrinsic dopants such as F or Sb to improve their electrical properties. However, the evolution of p-type TCOs possessing

sharp electric properties has trailed behind the evolution of such n-type TCOs, together with ITO (Indium Tin Oxide), Oxide, and AZO (Aluminum Oxide including Zinc) [3, 4]. In fact, attention to p-type-conductive SnO<sub>2</sub> has slowly grown within the latest years. SnO<sub>2</sub> has demonstrated to possess exceptionally brilliant n-type conductivity compared to Cu-based p-type metal oxides, to say nothing of other materials [5]. Consequently, the revelation regarding p-type conductivity within the compound may sign a crucial step within the manufacturing process of p-n junctions and far more obvious CMOS devices [6]. However, a huge debate has emerged regarding p-type doping TCOs, specifically SnO<sub>2</sub>, despite the considerable amounts of articles cleared the path regarding p-type successful doping SnO<sub>2</sub>,

as Watson and Scanlon declared the theory concerning advancement to be definitely one among the simplest factors regarding such development [7]. In fact, since Zunger and Kiliç published "the actually causes of conductivity and transparency surviving within SnO<sub>2</sub>," attention has grown toward natural shortcomings providing a SnO<sub>2</sub> n-type conductivity [8]. Increased investigation is demanded to look into improving n-type conductivity, versus fixing techniques within improving p-type conductivity by the utilization of compensative ways, regardless of evident permitting opposition to improving p-type conductivity by several ways [9]. In spite of a huge number associated with theories disclosed, presently a huge debate reigns regarding the ideally designed creation associated with donor defect worth increase to conductivity.

From our knowledge, actual research involving the prediction of results related to any environmental aspect during the film deposition process has not been carried out in SnO<sub>2</sub> yet. On the other hand, it could be possible that there is only an extremely tiny mention of compensatory methods in experimental-based research concerning the p-type doping of SnO<sub>2</sub>. Even though significant theoretical research has already been done concerning this subject, no actual experimental results have been generated concerning the influence of the environment in which the films are grown during doping performance and compensatory defect creation. These characteristics are assumed to have an essential influence upon the conductivity transition within materials. Besides Zn, Ga, In, and Al, Zn is also recognized as the most flexible cation acceptor doping element utilized within SnO<sub>2</sub> so far. It is a well-known fact that tin oxide exist in lot of different forms, like Sn-O, SnO<sub>2</sub> and even Sn<sub>3</sub>O<sub>4</sub> [10, 11]. In some instances, Zn dopant doped into SnO<sub>2</sub> has already been verified to raise n-type conductivity in addition to acceptor doping action characteristics [12]. It is most probable that the influence of the growth environment upon the SnO<sub>2</sub> device, with the aim of remaining initial with no doping followed by subsequent Zn doping, shall be explored. This research shall test acceptor defect behavior within conditions recognized as favorable with regard to

their creation, besides its influence upon the electric characteristics of the films developed. This is attributed to the fact that it permits control concerning the growth conditions surrounding the material. DFT is computationally much more efficient compared to other techniques such as Quantum Monte Carlo Simulations or Coupled Cluster Theory, although these are computationally intensive and produce very accurate results[13, 14]. For a material such as SnO<sub>2</sub> or any semiconductor/oxide, DFT can be useful in understanding details of electron density distribution, charge localization, and electron interaction. There are a number of DFT codes available, such as Wien2k, VASP, Quantum Espresso and others [14]. DFT is best suited for this research because of its computationally efficient and accurate calculation of material electronic structure properties for a material such as SnO<sub>2</sub>. It enables a thorough examination of material properties.

## II. METHODOLOGY

The electronic properties of SnO<sub>2</sub> were analyzed using the Density Functional Theory (DFT) code Wien2k, which is based on the Full Potential Linearized Augmented Plane Wave (FP-LAPW) method. The Exchange and Correlation part of the DFT functional was treated within the Generalized Gradient Approximation (GGA), using the Perdew-Burke-Ernzerhof (PBE) functional [15]. The GGA+U method was used in the calculations to approximate electron-electron interactions in the Sn 5s and 5p orbitals. The value of the Coulomb parameter U for the on-site Coulomb interaction in the GGA+U method was taken as [specify value of U] eV, based on the value used in previous literature [16, 17]. Before the electronic band-structure calculations were carried out, the SnO<sub>2</sub> unit cell and atomic positions were fully optimized by relaxing the cell parameters until the net atomic forces were less than [specify criterion, for instance, 0.01 mRy/Bohr]. The system optimization ensured that it is in the ground state configuration. The electronic band-structure calculations were done using the Monkhorst-Pack Brillouin zones subdivision method with [specify number] special k-points and an energy cut-off of [specify energy in eV]. The self-consistent field (SCF) calculations were also converged to an energy

tolerance. The band-structure calculations were performed in the high symmetry directions of the Brillouin zone, and attention was paid to how GGA+U corrections influence the band gap and electronic configuration of SnO<sub>2</sub>. The total density of states (DOS) of the system were also analyzed to determine the overall electronic band-structure, while the partial density of states (PDOS) for the Sn 5s and 5p as well as O 2p orbitals were analyzed to determine their contribution around the Fermi level. Additionally, the project density of states (PDOS) analysis helped in understanding the hybridization of the Sn 5s and O 2p orbitals, which is an indicator of the bond character of SnO<sub>2</sub>. Additionally, the charge density analysis helped in understanding how much of the charge is localized and how covalent or ionic the Sn-O bond is. Based on the above methodology, it became possible to

study the properties of SnO<sub>2</sub> at a level that focused on the influence of the GGA+U correction functional on the band gap and localization effects.

#### IV. RESULTS AND DISCUSSION

The electronic band structures of the parental and Sb doped SnO<sub>2</sub> (12.5%, 25% and 37.5%) compounds are shown in Fig. 1, with the high symmetry points in the Brillouin zone. To explain the effect of potentials XC, the complete density of states for the investigated compounds were found but using LDA and GGA techniques and mBJ (modified Becke-Johnson) potential. There are differences in the dispersion of the TDOS observed on LDA, GGA, and mBJ.

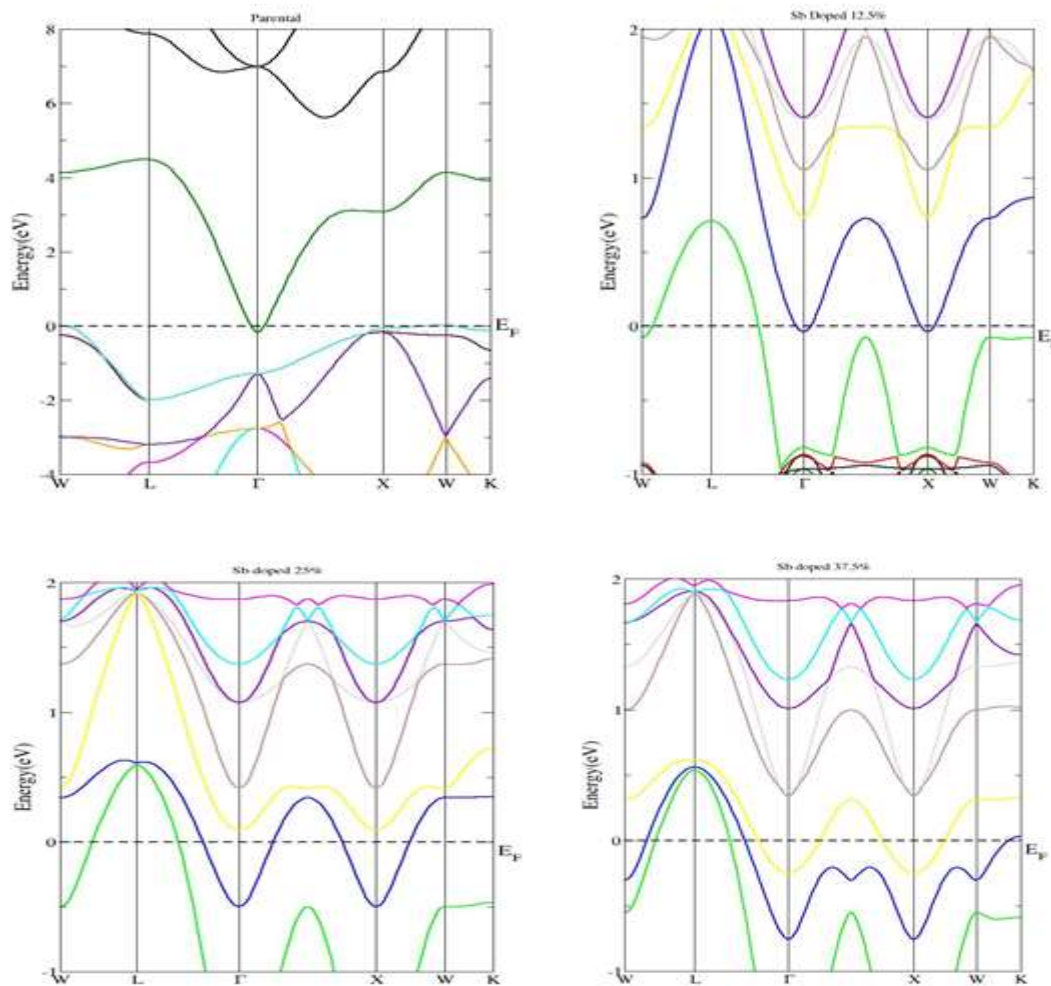


Fig 1. Electronic and structures of SnO<sub>2</sub> on different doping level

The differences are because of the fact that LDA and GGA are based on simple model assumptions that are rigid to regenerate the exchange correlation energy sufficiently and derivative of its charge space. The mBJ methodology can regenerate better exchange potential at the cost of less agreement in the exchange energy and yields better band splitting compared to LDA and GGA. Hence, we choose mBJ for more elaborations of the partial density of states (PDOS) of our selected compounds [18]. The information about the electronic structure and optical response is provided by material calculating band structure and fundamentals of it are directly associated to density of states.

The metallic nature of the compounds is revealed by computation of electronic band structures. The number of bands exceeding the Fermi level is also changed by changing the percentage of the dopant. 12.5% and 25% band structure shows that two band cross the Fermi level while 37.5 % band structure show that three bands crosses the Fermi level respectively. In the literatures to be contrast with our results, by due to successful application of FP-LAPW methods we discussed the performance of the energy band structure for these exacting materials under the present study [19, 20]. Following Fig. 1, the bands situated around the Fermi levels are due to the admixture of oxygen atom.

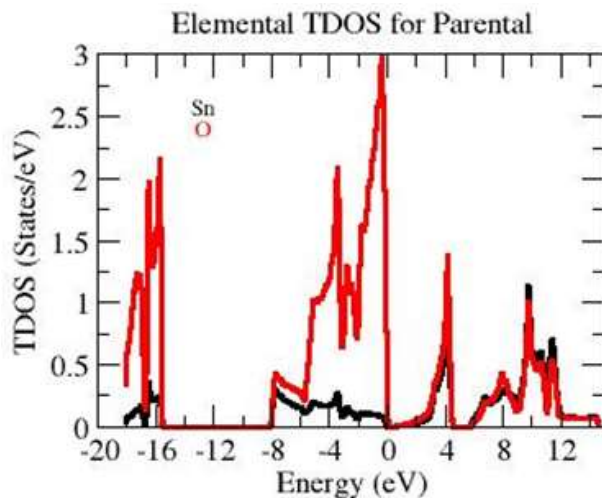


Fig 2. Elemental density of states for Sn and O

To highlight the nature of the electronic bands structure in greater extends, we enumerated the

total and partial density of states as shown in Fig.1 since we doped Sb atom, the nature of the material changes to metallic one and also the conductivity increases. The TDOS and EDOS (Fig. 2 and 3) for the compounds shows some similarities except the structure shift a bit towards lower energies of the valence band. We have found that over all the contribution occurs from Oxygen atom. There is a strong hybridization between the atoms of Sb and Sn. The total Density of State calculated at Fermi level  $N(E_F)$  is 10.3, 15.0 and 14.8 states/eV for 12.5, 25.0 and 37.5%, respectively. Metallic character can be clearly seen from the finite density of states at Fermi level [21]. The calculated density of states at the Fermi energy  $N(E_F)$  enables us to calculate the electronic specific heat coefficient, which is 1.78, 2.60 and 2.56 mJ/mol-K<sup>2</sup> for 12.5, 25.0 and 37.5%, respectively.

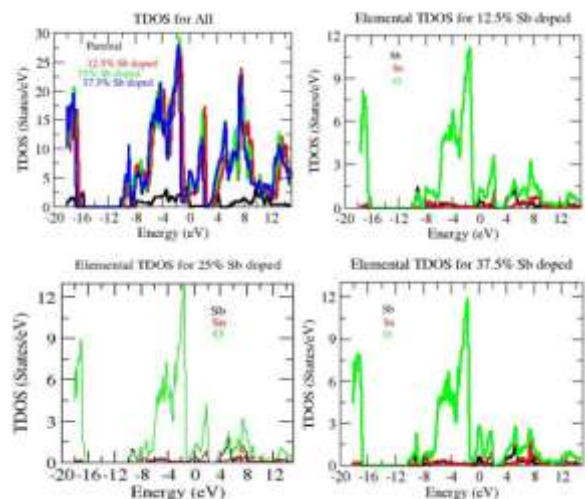


Fig 3. (a) Total density of states (b) TDOS for 12.5% Sb doped (c) TDOS for 25% Sb doped (d) TDOS for 37.5% Sb doped

To acknowledge and identify the nature of our material, the optical properties play an effective role. The important terms to describe the optical properties are dielectric constant  $\epsilon(\omega)$ , refractive index  $n(\omega)$ , reflectivity  $R(\omega)$ , Energy loss  $L(\omega)$ , absorption coefficient and real parts of the complex function. Dielectric function  $\epsilon(\omega)$  shows the interaction of photons with electrons and let the system to give response to electromagnetic radiations[22-24]. The dielectric function comprises

of two parts in which one part is real and 2nd one is imaginary. It can be expressed as

$$\epsilon(\omega) = \epsilon_1(\omega) + i\epsilon_2(\omega) \quad (3.1)$$

The imaginary part in the expression of dielectric function of three compounds is shown in Fig 4. Since the compound under investigation are of metallic behavior, therefore we took the intra-band transitions (Drude term) under consideration [19]. Where in eq. 3.3 represents mean plasma frequency and represents mean free time between the successive collisions [86

$$\epsilon_2(\omega) = \epsilon_{2inter}(\omega) + \epsilon_{2intra}(\omega) \quad (3.2)$$

$$\epsilon_{2intra}(\omega) = \frac{\omega_p^2 \tau}{\omega_1 + \omega_p^2 \tau^2} \quad (3.3)$$

The effect of Drude term is useful for the values less than 2.0 eV for 12.5, 25.0 and 37.5%, compounds. To calculate the dielectric function dependent on frequency we need electron wave function and energy eigenvalues of the state [25, 26]. Real and imaginary parts of dielectric function are important in study of optical spectra. The compound is symmetrically cubic in shape. The dielectric functions are as in eq. 3.4.

$$\epsilon^{xx}(\omega) = \epsilon^{yy}(\omega) = \epsilon^{zz}(\omega) \quad (3.4)$$

The general features of these compounds are not so similar due to the band structure differences. Therefore, there is difference in the optical spectra of the three compounds, which arises due to the doping of Sb percentage. We should highlight that substituting the Sb atom changes the heights of peaks, we conclude the 37.5% doped compound exhibits more metallic character than the 12.5 and 25% compounds. By using the Kramer's-Kronig relation [27], the real parts calculated is in Fig.4 (a-c). It is clear that the anisotropy among these compounds is weak.

The graph of the electron energy loss function of the investigated compounds is shown in Fig.4 (d). Prominent peaks are found at higher energies, which specify decrease in the reflectance. The reflectivity spectra for the investigated compounds are shown in fig 4 (e). The reflectivity spectra for all the compounds show almost the same behavior for the dopant materials. But the reflectivity spectra for the parental compound are a little higher than the

dopant compounds[28]. From the reflectivity spectra it is clear, that in the ultra violet regions it shows small reflectivity while higher in the visible region. It depicts that the material is a bad reflector [29]. The energy greater than 1.0 eV shows greater reflectivity of the compound, hence these material at the specific energies can be used as Bragg reflector.

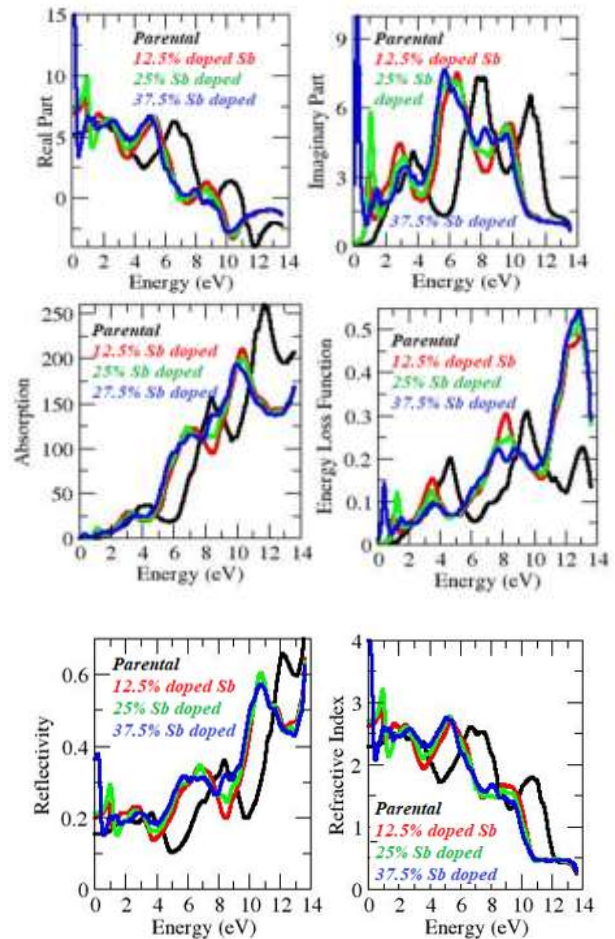


Fig 4 (a) Real part (b) Imaginary part (c) Absorption (d) Energy loss function (e) Reflectivity (f) Refractive index

## V. CONCLUSION

In order to summarize are results, We have analyzed the optical and electronic properties of the parental and Sb-doped SnO2 (12.5%, 25% and 37.5%) compound using the full potential linear augmented plane wave method within Wien2k code through DFT calculations. The band structure (BS) shows that the parental material has semiconducting nature,

while the nature of BS changes to metallic as we doped Sb. 12.5% and 25% band structure shows that two band cross the Fermi level while 37.5 % band structure show that three bands crosses the Fermi level respectively. From the density of states we found that the Oxygen atom dominates the Fermi level. The anisotropic behavior for parallel and perpendicular component of polarized electric field is studied. The imaginary and real parts of the complex function, refractive index, energy loss function and reflectivity are also studied.

#### Author contributions

**Awais Tabassum:** Conceptualization, Investigation, Methodology, Writing - Original Draft, Writing - Review & Editing. Muhammad Khizar Iqbal: Conceptualization, Supervision, Project administration, Resources, Writing - Review & Editing.

#### Declaration of competing interests

The authors declare that they have no known competing financial interests or personal relationships that could have appeared to influence the work reported in this study.

## REFERENCES

1. Hosono, H. and K. Ueda, Transparent conductive oxides, in Springer Handbook of Electronic and Photonic Materials. 2017, Springer. p. 1-1.
2. Stadler, A., Transparent conducting oxides—an up-to-date overview. *Materials*, 2012. 5(4): p. 661-683.
3. Patel, J., et al., A review of transparent conducting films (TCFs): Prospective ITO and AZO deposition methods and applications. *Nanomaterials*, 2024. 14(24): p. 2013.
4. Afre, R.A., et al., Transparent conducting oxide films for various applications: A review. *Reviews on advanced materials science*, 2018. 53(1): p. 79-89.
5. Habis, C., J. Zaraket, and M. Aillerie. Transparent conductive oxides. Part II. Specific focus on ITO, ZnO-AZO, SnO<sub>2</sub>-FTO families for photovoltaics applications. in *Defect and Diffusion Forum*. 2022. Trans Tech Publ.
6. Santra, S., et al., Mask-less deposition of Au-SnO<sub>2</sub> nanocomposites on CMOS MEMS platform for ethanol detection. *Nanotechnology*, 2016. 27(12): p. 125502.
7. Scanlon, D.O. and G.W. Watson, On the possibility of p-type SnO<sub>2</sub>. *Journal of Materials Chemistry*, 2012. 22(48): p. 25236-25245.
8. Kılıç, Ç. and A. Zunger, Origins of coexistence of conductivity and transparency in SnO<sub>2</sub>. *Physical review letters*, 2002. 88(9): p. 095501.
9. Kwok, C.K.G., et al., Conversion of p-type SnO to n-type SnO<sub>2</sub> via oxidation and the band offset and rectification of an all-Tin oxide pn junction structure. *Applied Surface Science*, 2023. 627: p. 157295.
10. Suman, P., et al., Comparative gas sensor response of SnO<sub>2</sub>, SnO and Sn<sub>3</sub>O<sub>4</sub> nanobelts to NO<sub>2</sub> and potential interferences. *Sensors and Actuators B: Chemical*, 2015. 208: p. 122-127.
11. Yu, X., et al., Recent progress on Sn<sub>3</sub>O<sub>4</sub> nanomaterials for photocatalytic applications. *International Journal of Minerals, Metallurgy and Materials*, 2024. 31(2): p. 231-244.
12. Sun, P., et al., Novel Zn-doped SnO<sub>2</sub> hierarchical architectures: synthesis, characterization, and gas sensing properties. *CrystEngComm*, 2012. 14(5): p. 1701-1708.
13. Shee, J., et al., On achieving high accuracy in quantum chemical calculations of 3 d transition metal-containing systems: a comparison of auxiliary-field quantum monte carlo with coupled cluster, density functional theory, and experiment for diatomic molecules. *Journal of chemical theory and computation*, 2019. 15(4): p. 2346-2358.
14. Ashraf, Z., et al., Ab-Initio Study of Electronic and Structural Properties for BaSnO<sub>3</sub> Compound Using DFT Calculations and FP-LAPW Technique in Wein2k Software. 2021.
15. Kabi, O., STRUCTURAL, ELECTRONIC, ELASTIC AND MAGNETIC PROPERTIES OF THE CeXO<sub>3</sub> (X= Cr, Ga) COMPOUNDS BY USING FP-LAPW METHOD. 2022, جامعة النجاح الوطنية.
16. Mishra, V. and S. Chaturvedi, Theoretical study of FCC-HCP phase coexistence and phase stability in Al by FP-LAPW method with GGA for exchange and correlation. *Physica B: Condensed Matter*, 2007. 393(1-2): p. 278-284.
17. Mesbahi, M., F. Serdouk, and M. Benkhedir, A DFT study of the electronic and optical

- properties of kesterite phase of  $\text{Cu}_2\text{ZnGeS}_4$  using GGA, TB-MBJ, and U exchange correlation potentials. *Acta Phys. Pol. A*, 2018. 134: p. 358-361.
18. Ponce, C., M. Caravaca, and R. Casali, Ab initio studies of structure, electronic properties, and relative stability of  $\text{SnO}_2$  nanoparticles as a function of stoichiometry, temperature, and oxygen partial pressure. *The Journal of Physical Chemistry C*, 2015. 119(27): p. 15604-15617.
  19. Ching-Prado, E., et al., Electronic structure and optical properties of  $\text{SnO}_2$ : F from PBE0 hybrid functional calculations. *Journal of Materials Science: Materials in Electronics*, 2018. 29(18): p. 15423-15435.
  20. Trani, F., et al., Density functional study of oxygen vacancies at the  $\text{SnO}_2$  surface and subsurface sites. *Physical Review B—Condensed Matter and Materials Physics*, 2008. 77(24): p. 245410.
  21. Duan, Y., Electronic properties and stabilities of bulk and low-index surfaces of  $\text{SnO}$  in comparison with  $\text{SnO}_2$ : A first-principles density functional approach with an empirical correction of van der Waals interactions. *Physical Review B—Condensed Matter and Materials Physics*, 2008. 77(4): p. 045332.
  22. Morris, A.J., et al., OptaDOS: A tool for obtaining density of states, core-level and optical spectra from electronic structure codes. *Computer Physics Communications*, 2014. 185(5): p. 1477-1485.
  23. Di Valentin, C. and G. Pacchioni, Spectroscopic properties of doped and defective semiconducting oxides from hybrid density functional calculations. *Accounts of chemical research*, 2014. 47(11): p. 3233-3241.
  24. Guo, D. and C. Hu, First-principles study on the electronic structure and optical properties for  $\text{SnO}_2$  with oxygen vacancy. *Applied surface science*, 2012. 258(18): p. 6987-6992.
  25. Canestraro, C.D., L.S. Roman, and C. Persson, Polarization dependence of the optical response in  $\text{SnO}_2$  and the effects from heavily F doping. *Thin Solid Films*, 2009. 517(23): p. 6301-6304.
  26. Borges, P.D., et al., DFT study of the electronic, vibrational, and optical properties of  $\text{SnO}_2$ . *Theoretical Chemistry Accounts*, 2010. 126(1): p. 39-44.
  27. Zak, A.K., A.M. Hashim, and J. Esmailzadeh, XPS studies and Kramers-Kronig analysis of the optical properties of  $\text{ZnO}/\text{SnO}_2$  nanocomposites synthesized by gelatin-based sol-gel method. *Optical Materials*, 2023. 142: p. 114111.
  28. Lee, J.-H., et al., Colored  $\text{MAPbI}_3$  perovskite solar cells based on  $\text{SnO}_2$ - $\text{SiO}_2$  distributed Bragg reflectors. *Materials Letters*, 2021. 282: p. 128828.
  29. Shen, C., et al.,  $\text{GaNN}$  light-emitting diodes with omni-directional reflector using nanoporous  $\text{SnO}_2$  film. *Chinese Optics Letters*, 2008. 6(2): p. 152-153.